International Journal of Scientific Research in Engineering and Management (IJSREM)
Volume: 08 Issue: 08 | Aug - 2024 SJIF Rating: 8.448 ISSN: 2582-3930

Uncertainty Analysis of Tensile Strength of Scarf Adhesive Joints Using Numerical Method

B. P. Sawant[1], P. P. Kulkarni[2]

1 Department of Mechanical Engineering & SKN Sinhgad College of Engineering, Korti,Pandharpur.
2 Department of Mechanical Engineering & SKN Sinhgad College of Engineering, Korti,Pandharpur.

Abstract - This study uses three-dimensional finite element (FE) analysis to investigate stress distribution and fatigue strength in adhesive scarf joints, which are complex due to their oblique geometry and varying material properties. ANSYS was used to model stress components within the adhesive and at the adhesive-adherent interface.

The FE models, created with eight-node solid elements, utilized fine meshing to ensure accurate stress representation. A mesh size of 0.025 mm was optimal. The models, assuming linearly elastic materials, were validated by comparing simulated deformations with experimental results. Findings enhance understanding of local stress states, improving adhesive joint design reliability.

Key Words: Adhesive scarf joints, finite element analysis, stress distribution, fatigue strength, ANSYS,

1.INTRODUCTION

Adhesive joints are critical components in many engineering applications due to their ability to bond different materials, distribute loads evenly, and reduce stress concentrations. Among the various types of adhesive joints, butt joints have been extensively studied because of their straightforward geometries and boundary conditions. These joints allow for relatively simple analytical solutions. However, the majority of previous analytical models have been two-dimensional, assuming plane strain conditions, which may not accurately represent the stress states in more complex joint configurations.

In contrast, scarf joints, characterized by their oblique geometry and the disparate material properties of the adherend-adhesive system, present significant analytical challenges. The oblique geometry introduces multiaxial loading conditions that complicate the stress analysis. Additionally, the adhesive boundary conditions at the specimen edges are intricate, further hindering the derivation of closed-form analytical solutions without substantial simplifications.

2. FE Meshes for All Types of Studied Specimens

The 2-D FEM calculations of scarf adhesive joints are represented by the model in Fig. 21. Both the upper and lower adherends are exposed to static tensile loadings and share the same materials and dimensions. The following boundary conditions are used: Tensile loading is applied to the end of the upper adherend, and the lower adherend is fixed in the y-direction. E1 and ν1 represent the adherends' Young's modulus and Poisson's ratio, while E2 and ν2 represent the adhesives. H1 stands for adherend length, w for adherend width, and 2t1 for adherend thickness. The symbols 2l and 2tn, respectively, stand for the adhesive's length and thickness.

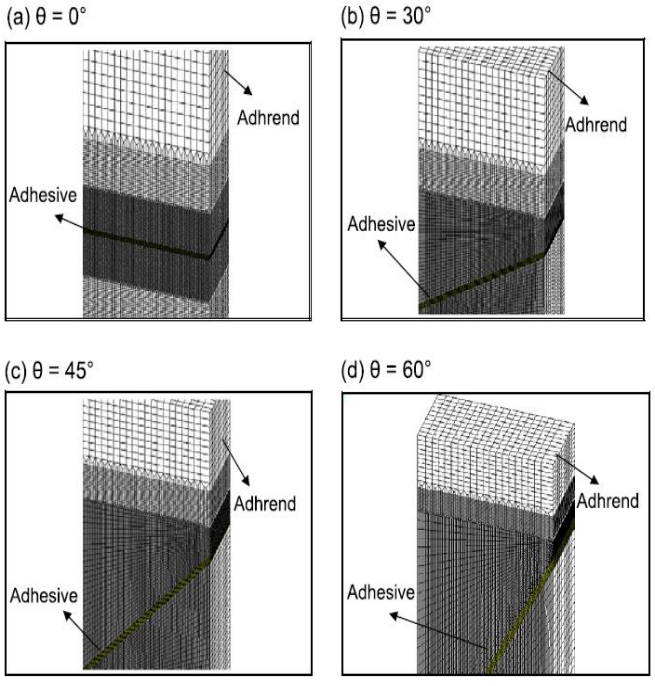

Fig -1: FE Meshes for All Types of Studied Specimens

3. Material Properties of the Adhesive and the Adherend in FE Analyses

Materials	Elastic modulus (MPa)	Poisson's ratio
SS 304	$193*10^3$	0.29
Epoxy Adhesive	29	0.35

Table -1: Material Properties of the Adhesive and the Adherend

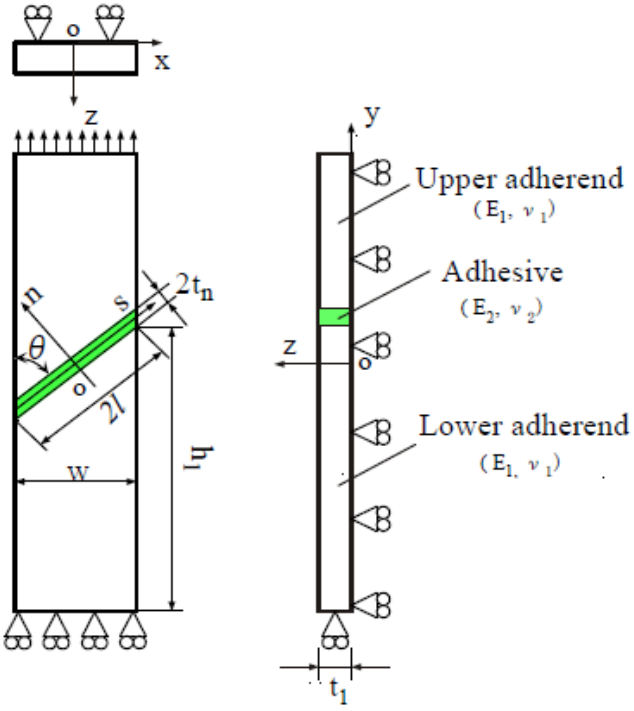

Fig-2: Model for 3-D FEM Calculations

The scarf adhesive joint mesh divisions in the three-dimensional finite element model calculations are illustrated in Fig. 22. It was determined that there would be 30256 total nodes and 27,000 total elements. The interfaces were selected to have the smallest element size of 5×5×5μm. The adherend material used was mild steel SS304, and the adhesive used was Araldite 420 A/B. To model the nonlinear constitutive relation for the adhesive and adherend materials, bi-linear material models were used in the FEM calculations.

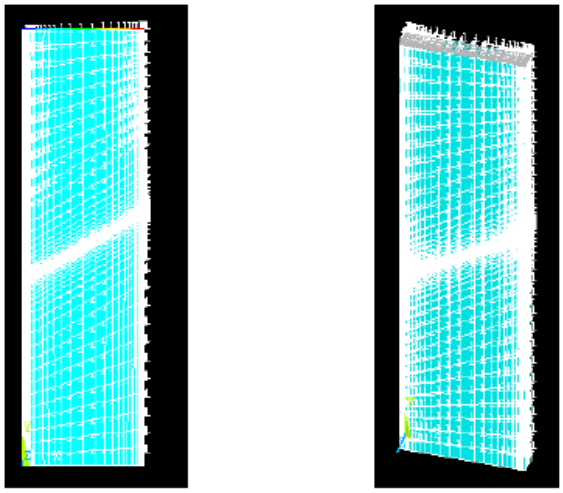

Fig-3: an example of mesh division of scarf adhesive joints in 2-D (a) and 3-D FEM calculations (b)

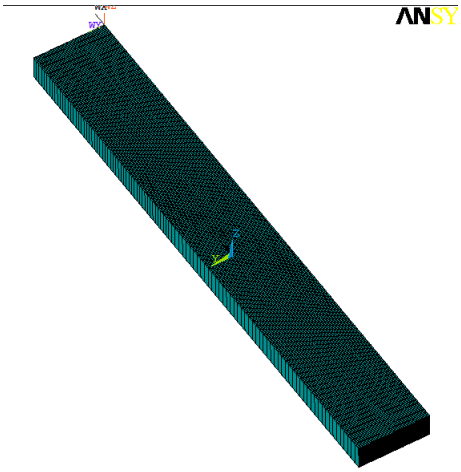

Fig-4: Mesh Divisions of Scarf Adhesive Joints

4. ANALYTICAL METHOD

Fig 5. shows the scarf adhesive joint mesh divisions in the calculations of the three-dimensional finite element model. It was calculated that there would be 27,000 total elements and 30256 total nodes. The interfaces with 5×5×5μm element sizes, the smallest possible, were chosen. Mild steel SS304 was the adherend material, and Araldite 420 A/B was the adhesive used. Bi-linear material models were employed in the FEM calculations to represent the nonlinear constitutive relation for the adhesive and adherend materials.

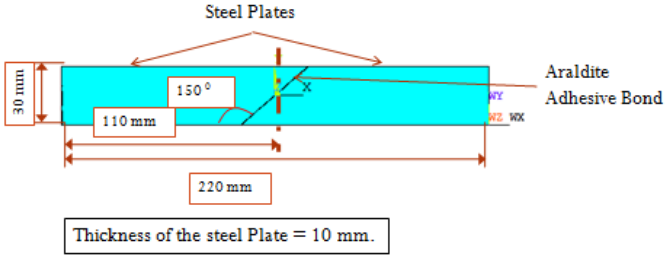

Fig-5: Dimensions of Adherends used in the Expe

(a) Meshes in 2-D

5. Analytical Results

5.1 Displacement Plot for Scarf Joint (30 Degree)

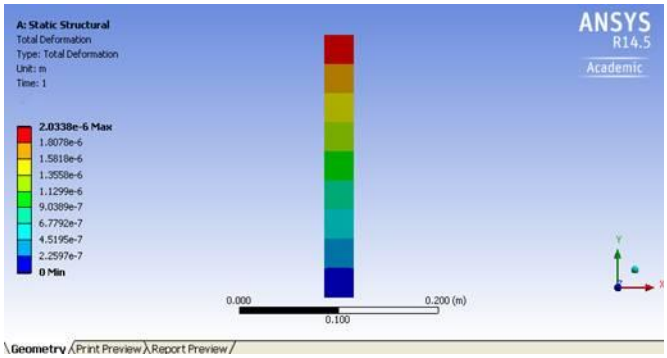

Fig-6 Displacement Plot for Scarf Joint 30 Degree

5.2 Displacement Plot for Scarf Joint (45 Degree)

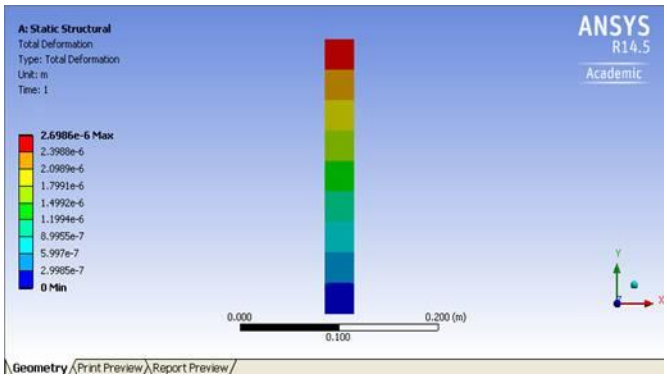

Fig-7 Displacement Plot for Scarf Joint 45 Degree

5.3 Displacement Plot for Scarf Joint (60 Degree)

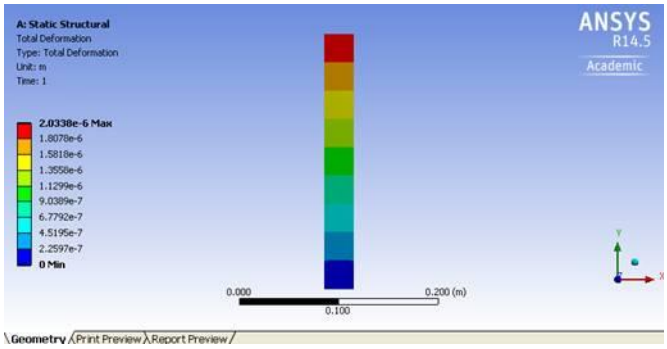

Fig-8 Displacement Plot for Scarf Joint 60 Degree

6. Results Summary for FEA of the Scarf Joint

Results Summary Table for FEA of the Scarf Joint			
Design	Force Applied (N)	Angle for the Scarf Joint	Max von Mises Stress in the joint Adhesive Layer (Mpa)
Design 1	509.6	30 Degrees	1.698
Design 2	676.2	45 Degrees	2.253
Design 3	764.4	60 Degrees	2.547

Table -2 Results Summary for FEA of the Scarf Joint

7. CONCLUSIONS

A conclusion that can be drawn from the above plotted result is that when the scarf angle increases, so does the Max von Mises Stress in the adhesive joint and the material's tensile strength. The testing point where crack initiation began was the maximum stress in the adhesive joint's stress distribution.

Experiments using the finite element method were conducted in ANSYS14 to analyse the breaking strength of scarf adhesive joints under tensile stresses. The results from ANSYS were confirmed to be similar to those obtained from a Universal Testing machine through a confirmation experiment.

8. REFERENCES

1. Midori Y. Pitanga, Maria Odila H. Cioffi, Herman J.C. Voorwald, Chun H. Wang ‘Reducing repair dimension with variable scarf angles’, international journal of adhesion and adhesive 104 (2021) 102752

2. Seshadri Matta, Ramji M. ‘Prediction of mechanical behaviour of adhesively bonded CFRP scarf jointed specimen under tensile loading using localised DIC and CZM’, International journal of adhesion and adhesive 89 (2019) 88–108

3. Ligang Sun, Ying Tie, Yuliang Hou, Xingxue Lu, Cheng Li ‘Prediction of failure behavior of adhesively bonded CFRP scarf joints using a cohesive zone model’, Engineering Fracture Mechanics 228 (2020) 106897

4. Jairaja Ra, and G Narayana Naik, ‘Numerical studies on weak bond effects in single and dual adhesive bonded single lap joint between CFRP and aluminium’, Materials Today: Proceedings 21 (2020) 1064–1068

5. J.E.S.M. Silva, R.D.S.G. Campilho, I.J. Sánchez-Arce, R.D.F. Moreira 'Numerical evaluation of tensile-loaded tubular scarf adhesive joints' Procedia Structural Integrity 41 (2022) 36–47

6. R.D.F. Moreira, M.F.S.F. de Moura, F.G.A. Silva, J.P. Reis, 'High-cycle fatigue analysis of adhesively bonded composite scarf repairs' Composites Part B 190 (2020) 107900

7. Francesco Marchione, Placido Munaf, 'Experimental strength evaluation of glass/aluminum double-lap adhesive joints' Journal of Building Engineering 30 (2020) 101284

8. Ligang Sun, Cheng Li, Ying Tie, Yuliang Hou, Yuechen DuanMarchione, Placido Munaf, 'Experimental and numerical investigations of adhesively bonded CFRP single-lap joints subjected to tensile loads' International Journal of Adhesion and Adhesives 95 (2019) 102402